European Journal of Immunology Clinical·Basic·Translational

Tissue immunology and leukocyte trafficking

Basic

Research Article

Nmes1 is a novel regulator of mucosal response influencing intestinal healing potential

Madeleine Hamley[#1,2], *Stephanie Leyk*[#1,2], *Christian Casar*[1,3], *Imke Liebold*[1,2], *Amirah Al Jawazneh*[1,2], *Clarissa Lanzloth*[1,2], *Marius Böttcher*[1], *Helmut Haas*[4], *Ulricke Richardt*[2], *Carla V. Rothlin*[5,6], *Thomas Jacobs*[2], *Samuel Huber*[1,7], *Lorenz Adlung*[1,7,8], *Penelope Pelczar*[1], *Jorge Henao-Mejia*[9] and *Lidia Bosurgi*[1,2,7]

[1] I. Department of Medicine, University Medical Center Hamburg-Eppendorf, Hamburg, Germany
[2] Protozoa Immunology, Bernhard Nocht Institute for Tropical Medicine, Hamburg, Germany
[3] Bioinformatics Core, University Medical Centre Hamburg-Eppendorf, Hamburg, Germany
[4] helminGuard, Sülfeld/Borstel, Germany
[5] Department of Immunobiology, Yale University School of Medicine, New Haven, Connecticut, USA
[6] Department of Pharmacology, Yale University School of Medicine, New Haven, Connecticut, USA
[7] Hamburg Center for Translational Immunology (HCTI), University Medical Center Hamburg-Eppendorf, Hamburg, Germany
[8] Center for Biomedical AI, University Medical Center Hamburg-Eppendorf, Hamburg, Germany
[9] The Institute for Immunology, Perelman School of Medicine, University of Pennsylvania, Philadelphia, Pennsylvania, USA

The initiation of tissue remodeling following damage is a critical step in preventing the development of immune-mediated diseases. Several factors contribute to mucosal healing, leading to innovative therapeutic approaches for managing intestinal disorders. However, uncovering alternative targets and gaining mechanistic insights are imperative to enhance therapy efficacy and broaden its applicability across different intestinal diseases. Here we demonstrate that *Nmes1*, encoding for *Normal Mucosa of Esophagus-Specific gene* 1, also known as *Aa467197*, is a novel regulator of mucosal healing. *Nmes1* influences the macrophage response to the tissue remodeling cytokine IL-4 *in vitro*. In addition, using two murine models of intestinal damage, each characterized by a type 2-dominated environment with contrasting functions, the ablation of *Nmes1* results in decreased intestinal regeneration during the recovery phase of colitis, while enhancing parasitic egg clearance and reducing fibrosis during the advanced stages of *Schistosoma mansoni* infection. These outcomes are associated with alterations in CX3CR1^{+} macrophages, cells known for their wound-healing potential in the inflamed colon, hence promising candidates for cell therapies. All in all, our data indicate *Nmes1* as a novel contributor to mucosal healing, setting the basis for further investigation into its potential as a new target for the treatment of colon-associated inflammation.

Keywords: Intestinal inflammation · Macrophages · Tissue remodeling · Type 2 cytokines

Additional supporting information may be found online in the Supporting Information section at the end of the article.

Correspondence: Dr. Lidia Bosurgi
e-mail: l.bosurgi@uke.de

[#]Madeleine Hamley and Stephanie Leyk contributed equally to this study.

Introduction

Macrophages have been extensively described as key contributors to each of the different phases of the wound healing response, from the early stage of coagulation and inflammation to tissue formation and finally tissue remodeling [1].

In the intestine, their function closely correlates with their specific localization. Macrophages in the lamina propria have a unique anti-inflammatory signature and fail to generate a proinflammatory response to TLR agonists [2]. When in contact with the lamina propria vasculature, macrophages are a barrier to bacterial pathogens and essential for vascular repair [3]. In the intestinal muscularis, macrophages are less prone to sensing perturbation from the lumen but facilitate neuroimmune interactions [4].

In the intestine, either resident macrophages or blood-derived monocytes express the CX3 chemokine receptor 1 (CX3CR1) [5]. High levels of CX3CR1 identify mucosal resident macrophages that control bacterial translocation to the lamina propria and exhibit an anti-inflammatory profile in homeostatic conditions [6, 7]. When transferred into a host, they alleviate colitis [8] and induce epithelial regeneration [9]. In a model of infectious colitis, $CX3CR1^{hi}$ macrophages express high levels of anti-inflammatory molecules such as *Il10* and *Tgfb1*, and of molecules associated with matrix remodeling [10]. In line with this, polymorphisms in the CX3CR1 gene in Crohn's disease patients correlate with a fibrostenosing disease [11, 12]. However, what regulates the anti-inflammatory function of $CX3CR1^{+}$ macrophages at a molecular level is still unknown.

The response to type 2 cytokines such as IL-4 and IL-13 regulates the tissue repair response in macrophages upon injury in many tissues. In line with this, the transfer of IL-4-treated macrophages in dinitrobenzene sulfonic acid (DNBS)-induced murine colitis leads to reduced disease severity and an increase in epithelial remodeling [13, 14]. Similarly, their transfer into prediabetic NOD mice protects them from developing type 1 diabetes [15] and ameliorates chronic renal disease in a model of adriamycin nephropathy [16]. These are only a handful of studies that provide direct evidence that reprogramming macrophages via IL-4 is an effective strategy to promote tissue remodeling in a variety of inflammatory settings. However, when an exacerbated or dysregulated type 2 cytokine-mediated repair process occurs, this can also contribute to the development of pathological fibrosis, as described in the context of chronic infections [17]. Therefore, a more comprehensive understanding of the mechanisms that regulate the macrophage response to type 2 cytokines is needed.

Here we show that *Nmes1*, normal mucosa of esophagus-specific gene 1 [18], also known as *Aa467197* and *C150rf48*, contributes to intestinal inflammation. *Nmes1* encodes for a small protein consisting of 83 amino acids. It is localized in the mitochondria [19, 20], and its mRNA transcript overlaps with the pre-miRNA sequence of the microRNA miR-147. In proinflammatory settings, miR-147 acts as a negative regulator of the inflammatory response upon stimulation of TLR2, TLR3, and TLR4 [19, 21]. Additionally, *Nmes1* has also been indicated as the most upregulated gene in monocyte-derived and tissue-resident macrophages in the peritoneal cavity upon treatment with IL-4 [22]. However, its function in the context of a type 2 immune response has not yet been determined. Our results indicate that *Nmes1* contributes to the macrophage response to IL-4 *in vitro*, controlling transcription of *Gata3*, *Ahr*, and molecules associated with the *Wnt* pathway. Additionally, in two distinct *in vivo* models of intestinal inflammation in which type 2 cytokines, such as IL-4 and IL-13, promote mucosal remodeling and favor the initiation and perpetuation of fibrotic disease, respectively [23–26], *Nmes1* regulates the regenerative/advanced stages of intestinal disease. This *Nmes1*-mediated modulation of mucosal responses is linked to changes in a subset of *Nmes1*-expressing $CX3CR1^{+}$ macrophages localized in the damaged intestine.

Results

Nmes1 influences the macrophage response to IL-4

Under IL-4 stimulation, *Nmes1* stands out as one of the most significantly upregulated genes in macrophages [22]. However, its role in a type 2 experimental setting has never been addressed.

Therefore, we first examined *Nmes1* expression in bone marrow-derived macrophages (BMDMs) by stimulating them with IL-4 *in vitro*. *Nmes1* expression increases 6 hours after stimulation and its expression decreases to basal levels between 12 and 72 h after treatment with IL-4 (Fig. 1A). Interestingly, expression of *Arg1*, *Retnla*, and *Chil3*, typical IL-4-induced tissue remodeling genes, peaks between 24h and 48h, with *Nmes1*, although only transiently expressed, preceding their induction (Fig. 1B). These data indicate that *in vitro, Nmes1* is induced in macrophages early after IL-4 stimulation.

To study the role of *Nmes1* in macrophages, we took advantage of a mouse model in which *Nmes1* is genetically ablated ($Nmes1^{-/-}$). First, we analyzed the macrophage differentiation capacity in $Nmes1^{-/-}$ mice and littermate controls ($Nmes1^{+/+}$). Neither differences in the number of hematopoietic pluripotent stem cells retrieved from the bone marrow at day 0 nor in the percentage of differentiated $CD11b^{+}F4/80^{+}$ macrophages and their proliferative capacity assessed via Ki-67 staining at different time points during M-CSF differentiation were detected between the two genotypes (Fig. 1C, Fig. S1). This indicates that *Nmes1* does not affect the differentiation of macrophages from the bone marrow per se. Additionally, no differences in polarization capacity between $Nmes1^{-/-}$ and $Nmes1^{+/+}$ BMDMs were observed upon IL-13 stimulation *in vitro*, while response to LPS treatment was altered in $Nmes1^{-/-}$ BMDMs compared controls, as previously described [21], suggesting that *Nmes1* is required for macrophage polarization under specific circumstances.

Second, to dissect whether *Nmes1* expression regulates the macrophage response to IL-4, we performed bulk RNA-sequencing (RNA-seq) on $Nmes1^{-/-}$ and $Nmes1^{+/+}$ BMDMs 6 and 24 h post-IL-4 treatment.

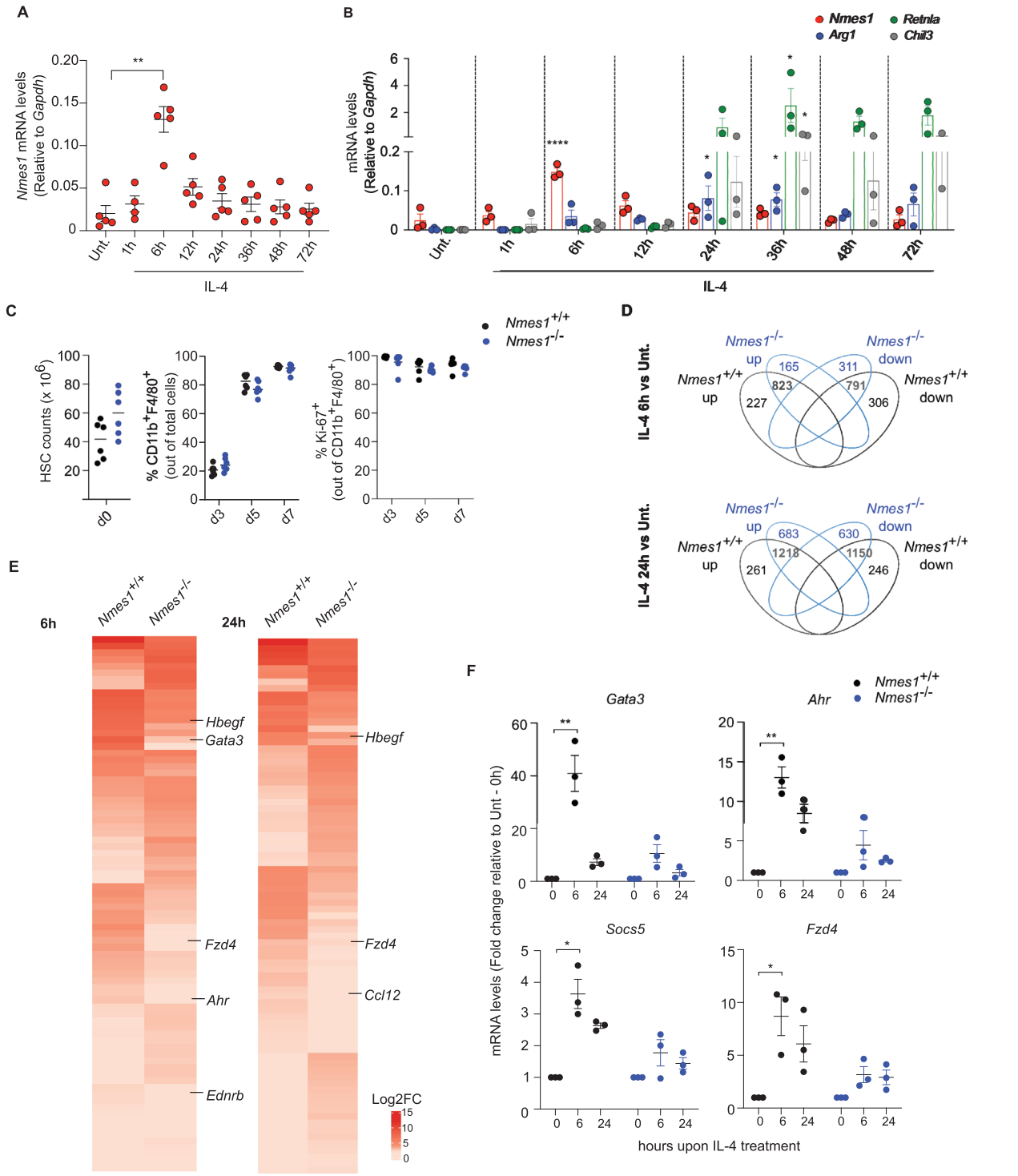

Figure 1. *Nmes1* influences the IL-4-induced tissue remodeling response in macrophages. Expression of (A) *Nmes1* or (B) various IL-4-induced genes, as detected by RT-qPCR, in bone marrow-derived macrophages (BMDMs) either untreated (Unt.) or treated with IL-4 for different incubation times. Data from two independent experiments (A), or one experiment representative of two (B) are shown. (C) Number of hematopoietic stem cells (HSCs) isolated from the bone marrow at day 0, frequency of macrophages, and their proliferation capacity (% Ki-67) in $Nmes1^{+/+}$ (black dots) and $Nmes1^{-/-}$ (blue dots) mice, during differentiation. (D) Venn diagram showing number of genes modulated in $Nmes1^{+/+}$ and $Nmes1^{-/-}$ BMDMs, treated with IL-4 for 6 or 24 h and compared with untreated (Unt.), as detected by bulk RNA-seq analysis. (E) Heat maps visualizing the first 80 genes (40 upregulated and 40 downregulated) differentially expressed in $Nmes1^{+/+}$ and $Nmes1^{-/-}$ BMDMs upon IL-4 treatment (log2 fold change ≥1.5 in 6 and 24 h IL-4-treated compared with the corresponding untreated and shared between $Nmes1^{+/+}$ vs. $Nmes1^{-/-}$ BMDMs). (F) Expression of indicated genes in $Nmes1^{+/+}$ vs. $Nmes1^{-/-}$ BMDMs treated with IL-4 for 6 or 24 h, as detected by RT-qPCR. Results are reported as fold change relative to the corresponding untreated (0 h) counterpart. One experiment is representative of two. (A, B, F) One-way ANOVA with Dunnett's multiple comparisons test (to the Unt. control). (C) Mann–Whitney *U* test (Comparing $Nmes1^{+/+}$ vs. $Nmes1^{-/-}$).

We first quantified the amount of unique and shared genes in IL-4-treated *Nmes1*$^{+/+}$ and *Nmes1*$^{-/-}$ macrophages, whose expression was modulated when compared with untreated cells (Fig. 1D). Next, we analyzed IL-4Ra protein levels by flow cytometry in *Nmes1*$^{+/+}$ vs *Nmes1*$^{-/-}$ BMDMs upon IL-4 stimulation. A similar pattern of expression suggests a similar ability to respond to IL-4 (Fig. S3). Second, as with our RNA-seq analysis, we selected genes with a log2 fold change ≥1.5 in 6 and 24 h IL-4-treated versus untreated macrophages and visualized the first 80 differentially expressed genes (DEGs) between *Nmes1*$^{+/+}$ and *Nmes1*$^{-/-}$ BMDMs in a heat map (Fig. 1E, Tables S1 and S2). Notably, *Arg1*, *Relma*, *Chil3*, and the haptoglobin–hemoglobin scavenger receptor *Cd163* did not appear among the top 80 DEGs. However, when considering the entire pool of analyzed transcripts, *Arg1* and *Cd163*, but not *Relma* or *Chil3*, were more highly induced in *Nmes1*$^{+/+}$ versus *Nmes1*$^{-/-}$ BMDMs 6 and 24 h after IL-4 stimulation. Moreover, transcription factors such as *Gata3* and *Ahr*, linked to the regulation of a tissue remodeling function in macrophages, were more highly induced in *Nmes1*$^{+/+}$ BMDMs compared with *Nmes1*$^{-/-}$ 6 h after IL-4 treatment. Similarly, Fzd4, a gene associated with the *Wnt* pathway, which operates in concert with IL-4 to promote the resolution of inflammation and/or mucosal repair upon intestinal damage or atherosclerosis [27–31], genes related to morphogenesis as well as to macrophages' anti-inflammatory status and angionesis capacity (*Ahr, Ednrb, Hbegf*) [32–34], and to monocyte chemotaxis (*Ccl12*) [35] were more highly induced in IL-4-stimulated *Nmes1*$^{+/+}$ BMDMs. RNA-seq data were validated via real-time quantitative PCR for some selected genes, including DEGs which were not directly incorporated into the heatmap (e.g. *Socs5*) [36] (Fig. 1F). Among them, only the differential expression of *Ahr* seems to persist in *Nmes1*$^{+/+}$ versus *Nmes1*$^{-/-}$ macrophages, 24 h after IL-4 treatment. (Fig. 1E). All together, these data suggest that in BMDMs, the response to IL-4 *in vitro* is influenced by *Nmes1*, and this, in turn, affects transiently key regulators of the type 2 immune response.

NMES1 is expressed in the murine and human colon and its mRNA levels are modulated during intestinal inflammation

We next analyzed the expression of *Nmes1* in the intestinal tissue. In homeostasis, high levels of *Nmes1* are specifically detectable in the mouse colon, independently of the gut microbiota (Fig. 2A). Likewise, in human tissue *NMES1* is expressed in the sigmoid colon from both healthy patients and people suffering from acute ulcerative colitis (UC) (Fig. 2B). Notably, *NMES1* expression increases during the remission phase of the disease while reduced IL-4 mRNA levels are detected only during the acute phase of the disease (Fig. 2B). In addition, analysis of a previously published single-cell transcriptomic dataset from ulcerated colon tissue from UC patients [37] reveals detection of *NMES1* in the different myeloid and lymphoid cell clusters, as represented in the t-distributed Stochastic Neighbor Embedding plot, with a trend toward higher *NMES1* expression in the monocyte/macrophage/dendritic cell cluster expressing CD14 (Fig. 2C, D). Expression of *CX3CR1* was also observed in this cluster (Fig. 2D). Interestingly, we observed a significant co-expression of *NMES1* and *CX3CR1* in CD14^{+} cells, suggesting this as the subpopulation of interest to study the role of *NMES1* during intestinal inflammation (Fig. 2E). Moreover, we correlated the expression of 958 individual genes, selected as macrophage marker genes or highly variable genes overall, against *NMES1* across all macrophage cells. Among the top correlating genes, we found many of them were associated with an anti-inflammatory/tissue-remodeling function in macrophages, including *IL10*, *TIMP1*, *MMP-9*, *MMP-12*, and *C1QB* (Fig. 2F).

These data suggest that *NMES1* is induced in the sigmoid colon of patients during the remission phase of UC. Furthermore, *NMES1* is expressed by multiple cell types, among them, a subcluster of intestinal CD14^{+} cells expressing CX3CR1 and characterized by an anti-inflammatory signature.

Nmes1 expression favors mucosal healing in a mouse model of DSS-induced colitis

Mice lacking IL-4 or the IL-4 receptor-α subunit exhibit milder acute-phase intestinal inflammation (day 3 and 7 of dextran sodium sulfate [DSS] ingestion), enhancing mucosal barrier function [38, 39]. However, IL-4 also has a protective role. IL-4-producing iNKT cells protect against colitis during the acute (7 days of DSS) and early remission phase (3 days after water provision) [40]. Similar protection in the early colitis phase (day 3 and 4) occurs with IL-4-polarized macrophages transferred 48 h before DNBS colitis induction [14, 40–42]. In the DSS-induced colitis model, *i.v*. injection of IL-4-treated macrophages on days 0 and 4 safeguards against colitis on day 7 [42]. All these data emphasize the critical role of IL-4 in the acute phase of the disease and in initializing the remission of the inflammation.

To investigate the role of *Nmes1* in the pathogenesis of colitis, we treated *Nmes1*$^{+/+}$ and *Nmes1*$^{-/-}$ mice with 1.5% DSS for 7 days, followed by 3–7 days of water. *Nmes1*$^{-/-}$ mice consistently showed a higher decrease in body weight compared with *Nmes1*$^{+/+}$ during the late phase of the disease, when tissue remodeling is triggered by the administration of normal water. However, no differences in colon length were detected (Fig. 3A, B). Colonoscopy in the *Nmes1*$^{-/-}$ mice revealed enhanced colitis, as demonstrated by increased granularity, loss of apparent vasculature, decreased translucency, and looser stool consistency (Fig. 3C). A trend toward increased ulceration, crypt hyperplasia, and cell infiltration was detected in *Nmes1*$^{-/-}$ compared with *Nmes1*$^{+/+}$ mice (Fig. 3D).

We next analyzed the expression of *Nmes1* in colon lamina propria cells during colitis. Both CD11b^{+}Ly6G^{-} myeloid cells and CD11b^{+}Ly6G^{+} neutrophils were enriched in the damaged tissue during the acute phase of the disease (d3–d7), while their frequency was reduced during the remission phase (d9–d14). Although the frequency of Ly6G^{-} myeloid cells was higher than

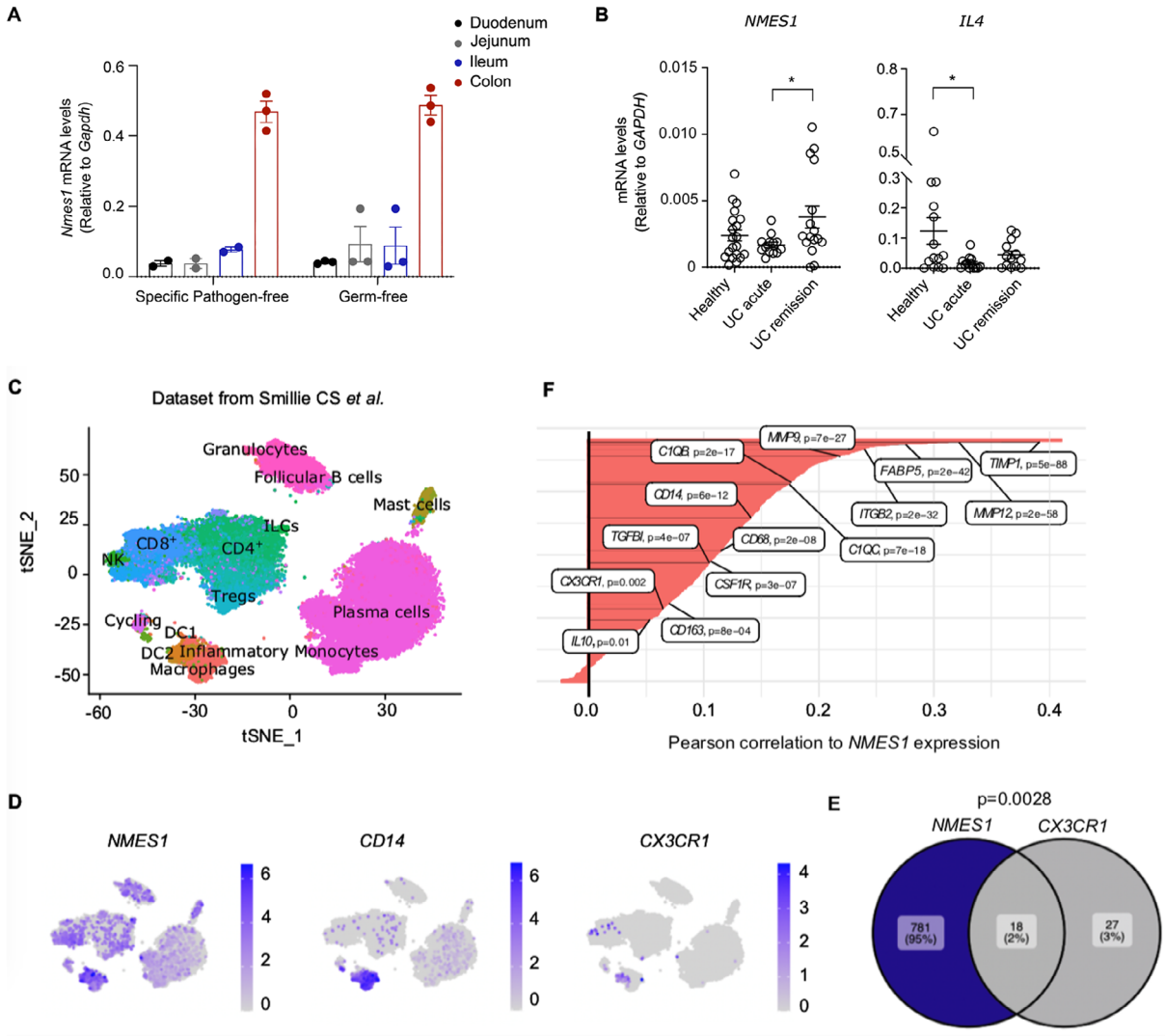

Figure 2. *NMES1* is expressed in murine and human colon. (A) Expression of *Nmes1*, detected by RT-qPCR, in the duodenum, jejunum, ileum, and colon of naïve WT mice housed differentially. One experiment representative of two is shown. (B) Levels of *NMES1* and *IL4* mRNA, as detected by RT-qPCR, in the sigmoid colon of either healthy patients, patients with acute ulcerative colitis, or in remission phase (n = 15–20). One-way ANOVA with Tukey's multiple comparisons test. (C) (upper panel) t-distributed Stochastic Neighbor Embedding plot of immune populations adapted from Smillie et al. [37]. (D) Normalized feature expression of *NMES1*, *CX3CR1*, and *CD14*. (E) VENN diagram of single- and double-positive cells for *NMES1* and *CX3CR1* within the CD14$^+$ cluster [37]. Hypergeometric test. (F) Pearson correlation of various anti-inflammatory genes to *NMES1* expression (*P*-value indicates the significance of Pearson correlation, adjusted for multiple testing).

neutrophils during the entire course of the DSS-induced colitis, neutrophils expressed higher levels of *Nmes1* during both the early and the advanced stage of the disease compared with the colonic lamina propria Ly6G$^-$ myeloid cells (Fig 3E, Fig. S4B).

We then quantified *Nmes1* mRNA levels by flow cytometry using PrimeFlow in the damaged colon. Among the CD45$^+$Ly6G$^-$CD11b$^+$ cells, we detected *Nmes1* mRNA mainly in a population of CD45$^+$CD11b$^+$F4/80^{dim} cells expressing various levels of CX3CR1 (Fig. S4D). We further confirmed the detection of *Nmes1* mRNA by RT-qPCR on FACS-sorted colonic CX3CR1$^+$ and CX3CR1$^-$ macrophages during the late phase of the disease (Fig. 3F, Fig. S4E). Additionally, CX3CR1$^+$ macrophages, which prevent susceptibility to DSS-induced colitis [6, 8, 43, 44], despite being present at a similar frequency in the two genotypes, showed reduced expression of a typical marker of IL-4-induced tissue remodeling, YM1 (protein encoded by *Chil3* gene), in *Nmes1*$^{-/-}$ mice compared with controls (Fig. 3G). These data indicate that *Nmes1* is expressed by a population of CX3CR1$^+$ colonic macrophages during the remission phase of colitis and appears to contribute to a proper wound-healing response.

Nmes1 expression promotes colon pathology in a mouse model of *Schistosoma mansoni* infection

We then employed a model of infection with the trematode helminth *Schistosoma mansoni*. The response to the infection is characterized by an initial type 1 response that later evolves

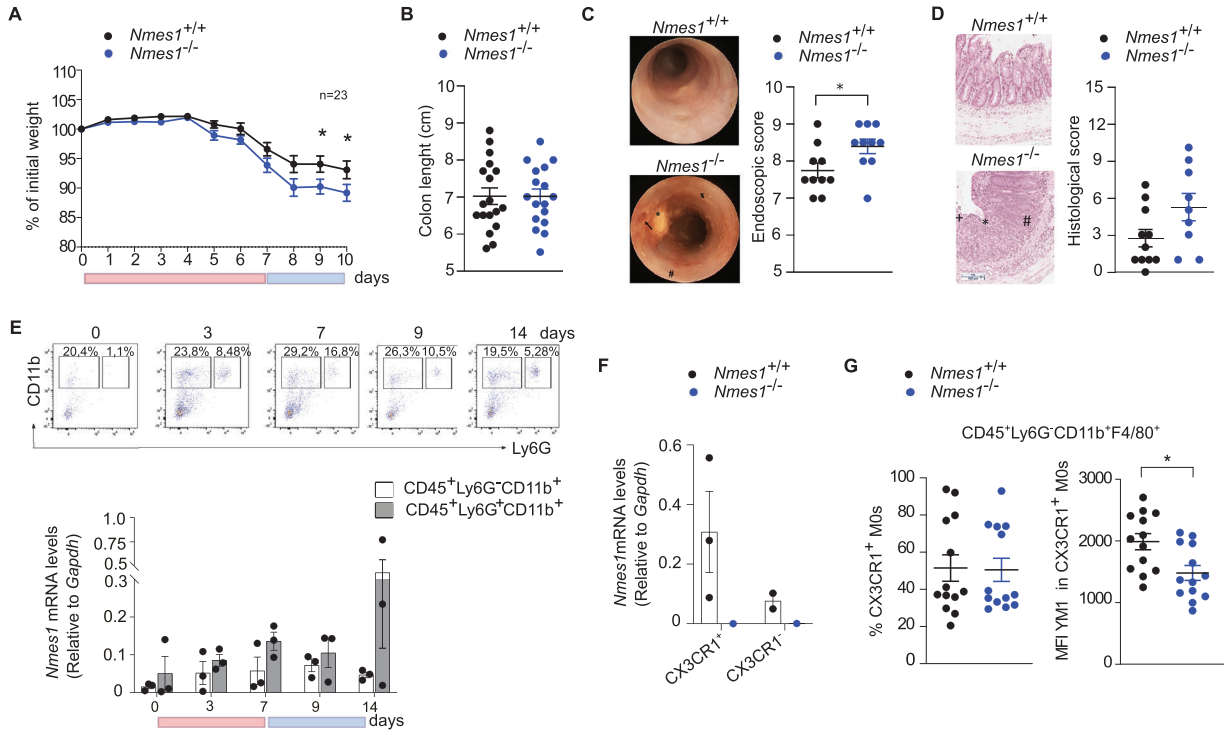

Figure 3. Genetic ablation of *Nmes1* leads to increased susceptibility to DSS-induced colitis. (A) Body weight, (B) colon length, (C) representative endoscopic images (asterisks, stool inconsistency; X, granularity; pound sign, abundant fibrin; arrow, ulceration) and endoscopic score of *Nmes1*$^{+/+}$ (black dots) and *Nmes1*$^{-/-}$ mice (blue dots). Data from two to three independent experiments are shown. (D) Representative images from H&E-stained colon sections (asterisks, ulceration; octothorpe, crypt hyperplasia; plus, neutrophil infiltration) and histological score (mean ± SEM). (E) (Upper panel) Representative FACS plots indicating the frequency of CD45$^+$Ly6G$^-$CD11b$^+$ myeloid cells and CD45$^+$CD11b$^+$Ly6G$^+$ neutrophils during the course of colitis. (Bottom panel) mRNA levels for *Nmes1* in FACS-sorted CD45$^+$Ly6G$^-$CD11b$^+$ and CD45$^+$CD11b$^+$Ly6G$^+$ isolated from the colon of DSS-treated WT mice, as reported in (A). Each dot corresponds to tissue pooled from three to six mice. (F) *Nmes1* mRNA amount in FACS-sorted CX3CR1$^+$ and CX3CR1$^-$ macrophages isolated from the colon of *Nmes1*$^{+/+}$ and *Nmes1*$^{-/-}$ mice. Three experiments with $n = 3$–6 mice pooled/genotype are shown. ND: not detectable. (G) Percentage of CX3CR1$^+$ macrophages (M0s) and MFI of YM1$^+$ in CX3CR1$^+$ M0s in *Nmes1*$^{+/+}$ and *Nmes1*$^{-/-}$ mice. Data from two independent experiments are shown. (A–D, G) Mann–Whitney *U* test. (B–D, F, G) Analysis performed on day 10 after DSS administration (7 days DSS+3 days water).

into a parasite antigen-driven type 2 response, enriched in IL-4 and IL-13 [23]. IL-4Ra signaling, although protective during the early phases of the infection, drives granulomatous and fibrosing inflammation against parasite eggs during the late phase of the disease [23, 45–47]. We observed an increase in *Nmes1* mRNA detected by flow cytometry on CX3CR1$^+$ colonic macrophages in *S. mansoni*-infected mice compared with naïve controls, with *Nmes1* mRNA also showing an increasing trend with aging (8, 14, and 21 weeks-old mice) (Fig. 4A)

CX3CR1$^+$ macrophages co-expressing tissue remodeling markers such as ARG-1, RELM-a, YM1, and CD206, also showed higher levels of *Nmes1* mRNA during *S. mansoni* infection compared with macrophages expressing lower levels of those tissue remodeling markers (Fig. 4B, Fig. S5A).

No differences in the amount of parasitic eggs were detected in the liver, as further confirmed by the similar ALT levels in *Nmes1*$^{+/+}$ and *Nmes1*$^{-/-}$ mice 14 weeks post infection with *S. mansoni* cercariae (Fig. 4C, Fig. S5B). Conversely, reduced egg count was detected in the colon of *Nmes1*$^{-/-}$ mice compared with *Nmes1*$^{+/+-}$ controls (Fig. 4C). To analyze whether this was the result of impairment in egg migration through the small and large intestine, the parasitic egg count in the ileum and in the colon was normalized to the number of eggs detected in the duodenum of each independent mouse. Our data indicate that in *Nmes1*$^{-/-}$ mice there was a significantly higher proportion of eggs in the ileum and colon compared with the duodenum (Fig. 4C), suggesting that *Nmes1* influences parasitic egg clearance/excretion from the small to the large intestine. In addition, analysis of collagen deposition mirroring the granuloma area via Picrosirius Red, and H&E staining to visualize the granuloma surrounding the parasitic eggs, strengthen our observation of lower egg numbers and consequently reduced granuloma in the colons of *Nmes1*$^{-/-}$ mice (Fig. 4D). Moreover, levels of *Timp1* and *Arg1*, considered one of the main mediators involved in fibrosis deposition during the chronic damage [48], were reduced in *Nmes1*$^{-/-}$ mice compared with controls. Similarly, reduced levels of *Il1b, Serpina3n*, whose expression correlates with pathological fibrosis [49], a trend toward reduced fibronectin (*Fn1*) and higher levels of *Col3*, a marker for a select subpopulation of colonic fibroblasts that make up the stem cell niche in the intestine [50], were detected in the intestine of *Nmes1*$^{-/-}$ versus *Nmes1*$^{+/+}$ infected mice (Fig. 4E).

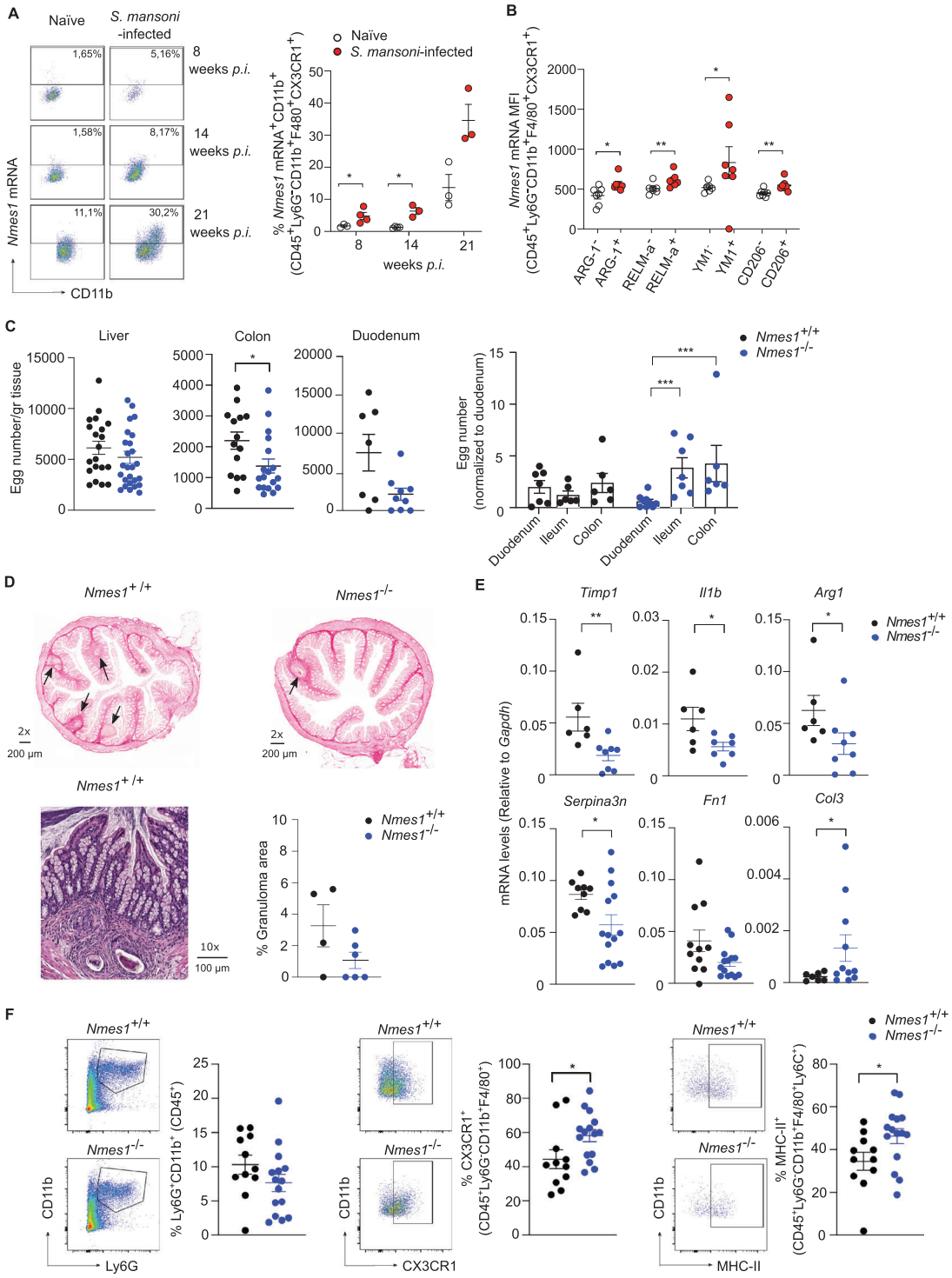

Figure 4. Genetic ablation of *Nmes1* confers protective immunity to *Schistosoma mansoni* infection. (A) Representative FACS plots and pooled data indicating frequency of *Nmes1*$^+$ in CX3CR1$^+$ macrophages detected via PrimeFlow, in the colon of naïve and *S. mansoni*-infected mice 8-, 14-, and 21-weeks post infection. (B) Mean fluorescence intensity for *Nmes1* mRNA detected in CD45$^+$Ly6G$^-$CD11b$^+$F4/80$^+$CX3CR1$^+$ colonic macrophages which express (red dots) or do not express (clear dots) different anti-inflammatory markers. One experiment is shown. (C) (Left) Number of *S. mansoni* eggs in the liver (n = 24–31), colon (n = 20–27), and duodenum (n = 7–9) of *Nmes1*$^{+/+}$ and *Nmes1*$^{-/-}$ mice. (Right) Ratio of egg count in the ileum and colon compared with the count in the duodenum of the corresponding mouse. (n = 7–9 mice). (D) Representative images of (upper panel) Picrosirius Red stain, with arrows indicating granulomas, and (bottom panel) H&E staining and quantification of SiRed-staining via ImageJ, in colon sections from *Nmes1*$^{+/+}$ (black dots) and *Nmes1*$^{-/-}$ (blue dots) mice. (E) mRNA from indicated genes detected in the colon of *Nmes1*$^{+/+}$ and *Nmes1*$^{-/-}$ mice. (F) Representative FACS plots (left) and pooled data (right) indicating frequency of CD11b$^+$Ly6G$^+$ neutrophils, CX3CR1$^+$ macrophages, and MHC-II$^+$Ly6C$^+$ macrophages in the colon of *Nmes1*$^{+/+}$ and *Nmes1*$^{-/-}$ mice. Data from three independent experiments are shown. In all the experiments presented, analysis was performed 14 weeks post infection with *S. mansoni*. (A–F) Mann–Whitney *U* test.

Interestingly, we did not observe differences in the frequency of $CD45^+CD4^+TCR\beta^+FOXP3^+CD25^+$ Tregs in *Nmes1*$^{-/-}$ and *Nmes1*$^{+/+}$ or alteration in the amount of type 2 cytokines such as IL-4 and IL-5 (Fig. S6), suggesting that *Nmes1* does not affect the regulatory response during the chronic phase of infection. In addition, no difference in the frequency of neutrophils, an increase in the frequency of $CX3CR1^+$ macrophages as well as macrophages with antigen presentation capacity ($MHC\text{-}II^+$) was detected in the damaged colon of *Nmes1*$^{-/-}$ vs *Nmes1*$^{+/+}$ mice (Fig. 4F, Fig. S5C). This emphasizes that *Nmes1* mainly impacts the innate arm of the host response and, among the cells analyzed, macrophages in particular.

Together, these data suggest that in a chronic disease such as infection with *S. mansoni*, where an exacerbated response to IL-4/IL-13 hampers wound healing [23–26], inhibiting *Nmes1* expression may aid in clearing parasitic eggs from the colon and promoting the re-establishment of intestinal homeostasis.

Discussion

Macrophages play a vital role in preventing disease progression and promoting tissue remodeling. In a model of DSS-induced colitis, they interact with colonic epithelial progenitors, supporting cell proliferation by factors like Wnt4 [31]. Similarly, the uptake of apoptotic cells by colonic macrophages aids monocyte maturation and restores intestinal homeostasis after damage [51–53]. Macrophages exposed to type 2 cytokines such as IL-4 exhibit a transcriptional response, mainly, but not only, associated with the acquisition of a wound healing profile. The regulation of IL-4-induced genes in macrophages, and the instant transcriptional response via STAT6 [54], continues to be under investigation. Among the further downstream signaling events, the expression of target proteins such as EGR2 has recently been proposed to regulate 40% of genes induced by IL-4 after 24 h, many of which are associated with cytokine production and signaling [55].

Notably, upon IL-4 stimulation, *Nmes1* stands out as one of the most significantly upregulated genes in macrophages [22]. Thus, the complete gap in knowledge regarding its function in the context of IL-4 guided us through the analysis presented here.

Interestingly, our data suggest that *Nmes1* is an early response gene to IL-4 stimulation *in vitro*, and although not affecting typical tissue remodeling genes in macrophages such as *Relma* and *Chil3*, it regulates the expression of a series of type 2-associated transcription factors such as *Ahr* and *Gata3*, which are associated with macrophage anti-inflammatory potential [32, 56]. In this scenario, it would be tempting to explore whether *Nmes1* complements molecules like *Egr2* in regulating macrophage signature profiles in response to type 2 cytokines.

Little is known about the function of *Nmes1* in the context of the proinflammatory setting [19, 21] and, to the best of our knowledge, no data has been reported on its role in the type 2 response. Published sequencing data highlight its potential influence on lung macrophage function [57] and its association with a population of macrophages present in the atherosclerosis plaque which originates from $CX3CR1^+$ monocyte precursors [58]. We have now extended these findings and have shown that *Nmes1* is expressed in a population of colonic $CX3CR1^+$ macrophages in a type 2-dominated environment. Interestingly, type 2 cytokines can drive both tissue remodeling in acute disease and fibrosis in chronic inflammation. In *Nmes1*$^{-/-}$ mice, this results in poorer mucosal healing during DSS-induced colitis recovery but fewer parasitic eggs and milder fibrosis during chronic *S. mansoni* infection. Further investigations should now be directed toward dissecting the contribution of additional cell types expressing *Nmes1* on the observed *in vivo* phenotypes, given that in different settings, *Nmes1* has been described as a marker for monocyte-derived effector DCs through proteomic analysis [59], and in proinflammatory neutrophils in the tumor microenvironment via single-cell sequencing [60]. Whereas activated DCs are suggested to contribute to intestinal pathology during colitis [61], neutrophils have a paradoxical role in colitis development, as they are critical for mucosal homeostasis, but their excessive recruitment and activation leads to extensive mucosal injury [62]. In the context of Schistosomiasis, DCs play a pivotal role in driving a type1/type 2 shift in the immune response when they interact with the parasitic egg antigens [63, 64], ultimately leading to the formation of schistosome egg granulomas [65]. Additional research focusing on these cell types during intestinal inflammation in *Nmes1*$^{-/-}$ mice, and the development of targeted conditional knockout transgenic mice for *Nmes1* could clarify the role of *Nmes1*-expressing macrophages in DSS-induced colitis and *S. mansoni* infection. In addition, these efforts could help to explore the plethora of signals inducing *Nmes1* activation in macrophages and its potential role in $CX3CR1^+$ macrophages in various diseases and tissues.

Nevertheless, despite the limitation of employing a total *Nmes1* knock-out mouse for our study, our findings may set the basis for a more profound grasp of $CX3CR1^+$ macrophage biology. This is especially crucial in the context of infections such as *S. mansoni*, where there is an imperative need for novel treatment strategies to enhance pathogen clearance and prevent the chronic form of the disease.

Materials and Methods

Mice

All mouse experiments were approved by the Office for Consumer Protection of the city of Hamburg (experiment protocols 66/17, N028/2023 and N042/2019, organ removal protocol O055/2018). Mice were bred and maintained in a specific pathogen-free facility at the Bernhard Nocht Institute for Tropical Medicine. For some experiments, WT mice were maintained in specific pathogen-free and germ-free facilities at the University Hospital Hamburg Eppendorf. Eight to twelve-week-old female mice were used for *in vivo* experiments and 8–12-week-old male mice were used for *in vitro* assays. *Nmes1*$^{-/-}$ mice were generated and kindly provided by Jorge Henao-Mejia (University of Pennsylvania).

Genotyping

gDNA was isolated from mouse ear tissue samples. *Nmes1* wild-type (~250 bp) and knockout (~150 bp) segments were amplified by PCR using the DreamTaq-Kit (Thermo Fisher) with the following primers:

Name	Sequence (5' to 3')
Nmes1 WT fwd	TCTATCGCTGCCTGTTTGTG
Nmes1 WT rev	CAAACCCGGAAGAGCTACTG
Nmes1 KO fwd	GCTTTCTGCGACTGTTGGAC
Nmes1 KO rev	ATGCAGGATCCAAAGAATGC

Bone marrow-derived macrophages

For differentiation into macrophages, hematopoietic pluripotent stem cells obtained from bone marrow suspension were plated in 10 mL RPMI containing 20% FCS, 30% L929 supplement, and 0.5% Gentamycin in a 10 cm petri dish at 37°C/5% CO_2 for 7 days. On day 3, half the media was replaced with fresh media. On day 5, the cells were split and incubated at 37°C/5% CO_2 for the remaining 2 days. On day 7, the cells were detached, counted, and used for further applications. All *in vitro* assays were performed under sterile conditions. Unless otherwise stated, cells were counted and seeded into wells of a 24-well plate at a concentration of 0.33×10^6 cells/well in 500 μL of appropriate medium. Cytokines were added to wells in the concentrations indicated in the individual experiments and the cells were incubated at 37°C/5% CO_2 for the indicated lengths of time before being processed for further analyses. Unless otherwise stated, recombinant IL-4 (Miltenyi) was added at a final concentration of 10 ng/mL.

DSS-induced colitis

Colitis was induced in mice by providing a 1.5% solution of DSS in place of drinking water for 5–7 days, followed by regular drinking water for 3–7 days. The maximum length of one experiment was 14 days. Mice were weighed and scored daily throughout each experiment. Mice were sacrificed at different time points during one experiment. Colons were removed and colon length was measured before the isolation of lamina propria cells for analysis using flow cytometry or FACS sorting.

Colonoscopy

Colonoscopy was performed in a blinded fashion for colitis scoring using the Coloview system (Karl Storz) as previously described [66] after mice were sacrificed. In brief, colitis was scored based on the granularity of the mucosal surface, vascular pattern, mucosal thickness, fibrin, and stool consistency (0–3 points for each parameter).

Histological analysis

Colon tissue was fixed in 37 % Formalin for 24 h followed by storage in PBS. Samples were processed, embedded, sectioned, and stained for Picrosirius Red and hematoxylin and eosin (H&E) at the Core Facility Mouse Pathology (University Medical Center Hamburg Eppendorf) following routine methods. Granulomatous areas in Picrosirius Red staining were calculated using ImageJ software. Each section was evaluated using a semiquantitative criterion-based method and scored as 0–5. The histopathological scores were assigned by a pathologist blinded to the experimental manipulation.

Preparation of single-sex male and female *S. mansoni* cercariae

S. mansoni cercariae preparation was obtained from *helmin*Guard (https://helminguard.de/). Briefly, to get single-sex cercariae, *Biomphalaria glabrata snails* (Brazilian strain) were individually exposed to one *S. mansoni* miracidium each. Upon patency (5 weeks after infection), the sex of the cercariae released from individual snails was determined by PCR. Separately, male and female cercariae-shedding snails were transferred to Petri dishes containing conditioned water and exposed to light for 2–4 h. Cercariae were passed through 50 and 20 μm filters, rinsed with remineralized distilled water, and recovered by rinsing the 20 μm filter backwards.

S. mansoni Infection

Mice were subcutaneously (s.c.) injected with 28–32 *S. mansoni* cercariae diluted in 200 μL distilled water. To count the cercariae, 10 μL cercariae solution was diluted in 100 μL distilled water in a 48-well plate with a grid. The cercariae were immobilized using 1 mL Lugol solution and counted under a light microscope. Mice were sacrificed at 8, 14, or 21 weeks post infection. Intestines, livers and blood were collected and processed for further analysis. In addition, colon tissue samples were taken and stored in RNAProtect (Qiagen) to analyze total RNA.

S. mansoni egg count

A piece of the left loop of the liver and a piece of the colon, ileum, and duodenum were harvested, weighed, and stored in 4% KOH solution for 8 or 16 h, respectively, at 37°C in a 24-well plate with a grid. The tissue was further disrupted by resuspending with a 1 mL pipette and the *S. mansoni* eggs were counted using a light microscope at 4× magnification. The eggs per gram liver/intestine were calculated. To evaluate egg migration through the intestine, in Fig. 3C (left panel), egg numbers in ileum and colon of each mouse were normalized to the egg count in the duodenum of the same mouse. Moreover, the values shown for the duodenum cor-

respond to the egg count in each mouse normalized to the average values.

Determination of ALT levels in the serum

Blood from *S. mansoni*-infected mice was collected in tubes containing 20 μL heparin, centrifuged and the serum stored at −20°C. The levels of alanine aminotransaminase (ALT) in the serum were then quantified via Reflotron (Roche). Measurements were performed at 25°C, using 32 μL of serum/mouse. Blood was collected in tubes containing 20 μL heparin, centrifuged, and the serum stored at −20°C.

Determination of cytokine levels in the serum

Cytokine concentrations in the serum of *S. mansoni*-infected mice were determined using LEGENDplex (Biolegend) according to the manufacturer's instructions. The LEGENDplex was measured at the Accuri C6 and analyzed with the LEGENDplex software v8.0.

Isolation of intestinal lamina propria cells

To isolate lamina propria cells, colons were removed from mice, cut open longitudinally, washed in PBS, cut into four to five smaller pieces, then incubated in 20 mL HBSS containing 200 μL EDTA 0.5 M per sample at 37°C in a shaker for 20 min to detach epithelial cells. After this first digestion, the colon pieces were washed in PBS three to five times to remove the epithelial cells. The remaining pieces were then minced to disrupt the tissue and digested in 5 mL HBSS containing 2% FCS, 3 μL DNaseI, and 5 mg collagenase VIII per sample for 45 min at 37°C on a shaker. After digestion, the suspension was mashed through a 100 μm cell strainer and then filtered again through a 40 μm cell strainer. The filtered suspension was centrifuged at 300 *g* for 5 min at 4°C to pellet the cells, which were then used for further applications.

Patient samples

RNA from total sigmoid colons of IBD patients was kindly provided by the University Clinic Hamburg-Eppendorf in Hamburg. For these samples, endoscopic biopsy specimens were obtained from the colon (sigma/rectum) from patients with UC (in acute or remission phase) or suspicion of intestinal disease (patients who were not diagnosed with IBD, here named healthy controls). An additional biopsy was taken from the largest foci of macroscopic inflammation. Human studies were approved by the local ethics committee (Ethik-Kommission der Ärztekammer Hamburg PV4444).

RNA isolation

Two methods were used for RNA isolation, depending on the application. For RNA samples sent for bulk RNA sequencing, samples were first lysed using the QiaShredder Kit (Qiagen), and RNA was isolated using the RNeasy Mini Kit (Qiagen). For all other applications, RNA was isolated from samples using phenol-chloroform extraction. For quantitative real-time PCR (qPCR), RNA retrotranscription was performed using the iScript cDNA Kit (BioRad). RT-qPCR was performed on a Corbett RotorGene (Corbett research/Qiagen), using the Maxima SYBR Green qPCR Master Mix (Thermo Fisher). All reactions were performed in duplicates, with *Gapdh* as reference gene, and analyzed using the Rotor-gene 6000 Series Software 1.7 (Corbett research/Qiagen).

Mouse primers:

Name	Sequence (5'–3')
Aa467197 fwd	GGAGCCACATCTTTCGCTTTG
Aa467197 rev	CTCCTCAACGGGCTTCCATTG
Ahr fwd	GGCTTTCAGCAGTCTGATGTC
Ahr rev	CATGAAAGAAGCGTTCTCTGG
Arg1 fwd	CATTGGCTTGCGAGACGTAGAC
Arg1 rev	GCTGAAGGTCTCTTCCATCACC
Chil3 fwd	CTGGAATTGGTGCCCCTACA
Chil3 rev	CAAGCATGGTGGTTTTACAGGA
Fzd4 fwd	TGCCAGAACCTCGGCTACA
Fzd4 rev	ATGAGCGGCGTGAAAGTTGT
Gapdh fwd	TCCCACTCTTCCACCTTCGA
Gapdh rev	AGTTGGGATAGGGCCTCTCTT
Gata3 fwd	GCTGGATGGCGGCAAAG
Gata3 rev	GTGGGCGGGAAGGTGAA
Il-1β fwd	GAAGAAGTGCCCATCCTCTG
Il-1β rev	AGCTCATATGGGTCCGACAG
Retnla fwd	CCAATCCAGCTAACTATCCCTCC
Retnla rev	CCAGTCAACGAGTAAGCACAG
Socs5 fwd	GACGGCTTAGTATCGAAGAA
Socs5 rev	GCTTATACAATGGGTTGACC
Timp1 fwd	GCGGTTCTGGGACTTGTGGGC
Timp1 rev	GCATCTCTGGCATCTGGCATC
Serpina3n fwd	CCTGATGCCCAGCTTTGAAA
Serpina3n rev	CCTGATGCCCAGCTTTGAAA
Fn1 fwd	GATGTCCGAACAGCTATTTACCA
Fn1 rev	CCTTGCGACTTCAGCCACT
Col3 fwd	GTTTACCTTCGCCTCACTAG
Col3 rev	TCTCTCCTTCCCAGGGCAAGCAT

Human primers:

Name	Sequence (5'–3')
GAPDH fwd	GCGAGATCCCTCCAAAATCAA
GAPDH rev	GTTCACACCCATGACGAACAT
NMES1 fwd	AGCTCATTCCCTTGGTGGTG
NMES1 rev	CAAAGGTGCTAAGGTTTGGGC
IL-4 fwd	ACTTTGAACAGCCTCACAGAG
IL-4 rev	TTGGAGGCAGCAAAGATGTC

Flow cytometry

Cells harvested from culture plates or isolated from mouse tissues were incubated with Fc-block (BioLegend, anti-CD16/CD32) diluted 1:10,000 in PBS + 2% FCS for 15 min at 4°C prior to the staining. For the staining of surface epitopes, cells were incubated with the antibody cocktail for 45 min at 4°C in the dark. If intracellular epitopes were analyzed, cells were fixed (2% PFA) and permeabilized (BD Perm/Wash) for 15 min at RT before staining. Cells were stained and fluorescence was measured on an LSRII (BD Biosciences). Data were analyzed with the FlowJo software (Tree Star).

List of antibodies:

Epitope	Fluorochrome	Clone	Company
CD11b	APC/Cy7 BV510 FITC	M1/70	Biolegend
CD45	BV510 PE/Cy7	30-F11	Biolegend
CX3CR1	AF700 PE/Cy7	SA011F11	Biolegend
F4/80	APC/Cy7 AF700 FITC	BM8	Biolegend
Ly6G	APC/Cy7 BV421 PerCP-Cy5.5	IA8	Biolegend
a-goat IgG	FITC	Poly4606	Invitrogen, Gibco
CD4	BV605	GK1.5	Biolegend
TCRβ	APC	H57-597	Biolegend
FOXP3	AF488	150D	Biolegend
CD25	AF700	PC61	Biolegend
a-rabbit IgG	BV421 BV510	Poly4064	Biolegend
ARG1	APC PE	A1exF5	Invitrogen, Gibco
RELMa		Polyclonal rabbit IgG	PeproTech GmbH
Ym1		Polyclonal goat IgG	R&D Systems
Live/dead fixable blue			ThermoFisher Scientific

PrimeFlow

The PrimeFlow RNA assay is an in situ hybridization assay that was used to analyze the expression of *Nmes1* mRNA via flow cytometry. The assay was performed in 96-well plates according to the manufacturer's instructions. All wash steps were performed twice with PrimeFlow wash buffer (wash buffer) and centrifugation at 1000*g* for 4 min at room temperature. Target probes were diluted 1:20 in the provided target probe diluent, and provided label probes were diluted 1:100 in the provided label probe diluent. After extracellular staining, fixation, permeabilization, and intracellular staining, cells were washed and incubated with 100 μL wash buffer and 100 μL diluted target probe for 2 h at 40°C in an incubator. Afterward, cells were washed and incubated with 100 μL wash buffer and 100 μL of the provided PreAmp mixture for 1.5 h at 40°C. After washing, this step was repeated using 100 μL wash buffer and 100 μL of the provided Amp mixture. After washing, cells were incubated with 100 μL wash buffer and 100 μL diluted label probe for 1 h at 40°C. Finally, cells were washed and resuspended in FACS buffer for acquisition at the LSR II flow cytometer.

PrimeFlow target probes:

Construct	Colour type	Company
Aa467197	Type 1 (AF647)	Thermo Fisher Scientific
B2m	Type 6 (AF750)	Thermo Fisher Scientific

Cell sorting

Cells were labeled with the antibodies of choice through extracellular staining and FACS-sorted by the core facility of the BNITM using a BD FACSAria cell sorter. Prior to sorting, cells were filtered through a 30 μm cell strainer. The sorting of cells was performed using a 70 μm nozzle. Sorted cells were collected in a cold FACS measurement buffer.

Bulk RNA sequencing

BMDMs differentiated from *Nmes1*$^{+/+}$ and *Nmes1*$^{-/-}$ mice were either untreated or treated with 10 ng/ml of IL-4 for 6 or 24 h. RNA was then isolated via the RNeasy Mini Kit from BMDMs differentiated from three mice pooled/condition. RNA sequencing was performed by BGI (BGI TECH SOLUTIONS, Hongkong). Library preparation and transcriptome sequencing were performed using 100 base/paired-end reads on BGI's DNBSEQ Technology Platform.

STAR (v2.7.6a) [67] was used to align the raw read against the mouse reference genome GRCm38 (Ensembl 100). Differential expression analysis was performed in R (version 4.0, R Core Team) using edgeR (version 3.32.0) [68]. Only genes with a count per million value >1 in at least one sample were included in the analysis. We followed the edgeR authors' recommendation for experiments with no replicates and defined a fixed biological coefficient of variation of 0.1, that is, setting dispersion in the exactTest to 0.1^2. An FDR <0.05 was defined as the threshold for DE genes.

For the downstream analysis, genes with a log2 fold change ≥1.5 after incubation with IL-4 at 6 or 24 h compared with the corresponding untreated cells were selected. Of these genes, those shared between *Nmes1*$^{+/+}$ and *Nmes1*$^{-/-}$ cells were compared

and displayed in a heatmap. These genes were selected by calculating the ratio between the *Nmes1*$^{+/+}$ and *Nmes1*$^{-/-}$ cells log2 fold changes and selecting the 40 genes with the smallest and largest ratios respectively.

Sequencing data

Data from Smillie et al. [37] were accessed and downloaded through the Single Cell Portal: SCP259 (https://portals.broadinstitute.org/single_cell). Data were processed with R version 3.6, and annotated as previously described [18]. For the detection of NMES1^{+} and CX3CR1^{+} CD14^{+} cells, normalized expression >0 was considered.

Statistics

Statistical analysis and comparison were performed using Prism 9 (GraphPad). When multiple comparisons to a control were performed, ordinary one-way ANOVA with Dunnett's multiple comparisons test was used. If normally distributed, analysis was performed using ordinary one-way ANOVA with Tukey's. When a comparison between two groups was performed, a Mann–Whitney *U* test was used. A *P*-value $\leq$ 0.05 was considered statistically significant ($^{*}P \leq 0.05$, $^{**}P < 0.01$, $^{***}P < 0.001$, $^{****}P < 0.0001$). Data points without specific labels are indicative of nonstatistically significant results. Data are shown as mean $\pm$ SEM. Unless stated in the legend, each data point indicates one independent sample.

Acknowledgements: The authors thank all the members of the Bosurgi laboratory for technical support and helpful discussions. The authors also thank Birgit Huesing and Christiane Steeg for technical support during FACS sorting, Francesco Siracusa for advice on regulatory T cell analysis, and the Animal Care Staff at the Bernhard Nocht Institute for Tropical Medicine for support with animal experimentation. Graphical abstract was created with BioRender.com. This study was supported by grants from Werner Otto Stiftung (to LB), Landesfoschungsförderung Hamburg, LFF-FV74 (to LB), and Pro Exzellenzia Plus (to SL).
Open access funding enabled and organized by Projekt DEAL.

Conflict of interest: Helmut Haas is the head and owner of *helmin*Guard. The remaining authors declare no conflict of interest

Author contributions: Madeleine Hamley, Stephanie Leyk, and Lidia Bosurgi conceived and planned the experiments and analyzed and interpreted the data. Madeleine Hamley, Stephanie Leyk, Imke Liebold, Amirah Al Jawazneh, Clarissa Lanzloth, Ulricke Richardt, and Penelope Pelczar performed the experiments. Christian Casar and Lorenz Adlung applied computational techniques for data analysis. Marius Böttcher analyzed and scored histological sections. Helmut Haas provided *S. mansoni* cercariae. Jorge Henao-Mejia provided *Nmes1*$^{-/-}$ mice. Lidia Bosurgi conceived the study and wrote the manuscript. Madeleine Hamley, Stephanie Leyk, Christian Casar, Imke Liebold, Amirah Al Jawazneh, Clarissa Lanzloth, Marius Böttcher, Helmut Haas, Ulricke Richardt, Carla V. Rothlin, Thomas Jacobs, Samuel Huber, Lorenz Adlung, Penelope Pelczar, Jorge Henao-Mejia, and Lidia Bosurgi reviewed the results and approved the final manuscript.

Data availability statement: Datasets reporting RNA sequencing on BMDMs from *Nmes1*$^{-/-}$ or control counterparts, either untreated or treated with IL-4 are deposited in publicly available repositories in ArrayExpress under the accession number E-MTAB-13522. Further data that support the findings of this study are available from the corresponding author upon request.

Peer review: The peer review history for this article is available at https://publons.com/publon/10.1002/eji.202350434.

References

1 **Minutti, C. M., Knipper, J. A., Allen, J. E. and Zaiss, D. M. W.**, Tissue-specific contribution of macrophages to wound healing. *Semin. Cell Dev. Biol.* 2017. **61**: 3–11.

2 **Denning, T. L., Wang, Y.-C., Patel, S. R., Williams, I. R. and Pulendran, B.**, Lamina propria macrophages and dendritic cells differentially induce regulatory and interleukin 17-producing T cell responses. *Nat. Immunol.* 2007. **8**: 1086–1094.

3 **Honda, M., Surewaard, B. G. J., Watanabe, M., Hedrick, C. C., Lee, W.-Y., Brown, K., Mccoy, K. D. et al.**, Perivascular localization of macrophages in the intestinal mucosa is regulated by Nr4a1 and the microbiome. *Nat. Commun.* 2020. **11**: 1329.

4 **Gabanyi, I., Muller, P. A., Feighery, L., Oliveira, T. Y., Costa-Pinto, F. A. and Mucida, D.**, Neuro-immune interactions drive tissue programming in intestinal macrophages. *Cell* 2016. **164**: 378–391.

5 **Jung, S., Aliberti, J., Graemmel, P., Sunshine, M. J., Kreutzberg, G. W., Sher, A. and Littman, D. R.**, Analysis of fractalkine receptor CX(3)CR1 function by targeted deletion and green fluorescent protein reporter gene insertion. *Mol. Cell Biol.* 2000. **20**: 4106–4114.

6 **Medina-Contreras, O., Geem, D., Laur, O., Williams, I. R., Lira, S. A., Nusrat, A., Parkos, C. A. et al.**, CX3CR1 regulates intestinal macrophage homeostasis, bacterial translocation, and colitogenic Th17 responses in mice. *J. Clin. Invest.* 2011. **121**: 4787–4795.

7 **Zigmond, E., Varol, C., Farache, J., Elmaliah, E., Satpathy, A. T., Friedlander, G., Mack, M. et al.**, Ly6C hi monocytes in the inflamed colon give rise to proinflammatory effector cells and migratory antigen-presenting cells. *Immunity* 2012. **37**: 1076–1090.

8 **Kayama, H., Ueda, Y., Sawa, Y., Jeon, S. G., Ma, J. S., Okumura, R., Kubo, A. et al.**, Intestinal CX3C chemokine receptor 1(high) (CX3CR1(high)) myeloid cells prevent T-cell-dependent colitis. *Proc. Natl. Acad. Sci. USA* 2012. **109**: 5010–5015.

9 **Murai, M., Turovskaya, O., Kim, G., Madan, R., Karp, C. L., Cheroutre, H. and Kronenberg, M.**, Interleukin 10 acts on regulatory T cells to maintain

expression of the transcription factor Foxp3 and suppressive function in mice with colitis. *Nat. Immunol.* 2009. **10**: 1178–1184.

10 **Koscsó, B., Kurapati, S., Rodrigues, R. R., Nedjic, J., Gowda, K., Shin, C., Soni, C. et al.**, Gut-resident CX3CR1(hi) macrophages induce tertiary lymphoid structures and IgA response in situ. *Sci. Immunol.* 2020. **5**.

11 **Brand, S., Hofbauer, K., Dambacher, J., Schnitzler, F., Staudinger, T., Pfennig, S., Seiderer, J. et al.**, Increased expression of the chemokine fractalkine in Crohn's disease and association of the fractalkine receptor T280M polymorphism with a fibrostenosing disease Phenotype. *Am. J. Gastroenterol* 2006. **101**: 99–106.

12 **Sabate, J.-M., Ameziane, N., Lamoril, J., Jouet, P., Farmachidi, J.-P., Soulé, J.-C., Harnois, F. et al.**, The V249I polymorphism of the CX3CR1 gene is associated with fibrostenotic disease behavior in patients with Crohn's disease. *Eur. J. Gastroenterol Hepatol* 2008. **20**: 748–755.

13 **Jayme, T. S., Leung, G., Wang, A., Workentine, M. L., Rajeev, S., Shute, A., Callejas, B. E. et al.**, Human interleukin-4-treated regulatory macrophages promote epithelial wound healing and reduce colitis in a mouse model. *Sci. Adv.* 2020. **6**: eaba4376.

14 **Leung, G., Petri, B., Reyes, J. L., Wang, A., Iannuzzi, J. and Mckay, D. M.**, Cryopreserved Interleukin-4-treated macrophages attenuate murine colitis in an integrin beta7 - dependent manner. *Mol. Med.* 2016. **21**: 924–936.

15 **Parsa, R., Andresen, P., Gillett, A., Mia, S., Zhang, X.-M., Mayans, S., Holmberg, D. et al.**, Adoptive transfer of immunomodulatory M2 macrophages prevents type 1 diabetes in NOD mice. *Diabetes* 2012. **61**: 2881–2892.

16 **Wang, Y., Wang, Y. P., Zheng, G., Lee, V. W. S., Ouyang, L., Chang, D. H. H., Mahajan, D. et al.**, Ex vivo programmed macrophages ameliorate experimental chronic inflammatory renal disease. *Kidney Int.* 2007. **72**: 290–299.

17 **Gieseck, R. L., Wilson, M. S. and Wynn, T. A.**, Type 2 immunity in tissue repair and fibrosis. *Nat. Rev. Immunol.* 2018. **18**: 62–76.

18 **Zhou, J., Wang, H., Lu, A., Hu, G., Luo, A., Ding, F., Zhang, J. et al.**, A novel gene, NMES1, downregulated in human esophageal squamous cell carcinoma. *Int. J. Cancer* 2002. **101**: 311–316.

19 **Clayton, S. A., Daley, K. K., Macdonald, L., Fernandez-Vizarra, E., Bottegoni, G., O'neil, J. D., Major, T. et al.**, Inflammation causes remodeling of mitochondrial cytochrome c oxidase mediated by the bifunctional gene C15orf48. *Sci. Adv.* 2021. **7**: eabl5182.

20 **Floyd, B. J., Wilkerson, E. M., Veling, M. T., Minogue, C. E., Xia, C., Beebe, E. T., Wrobel, R. L. et al.**, Mitochondrial protein interaction mapping identifies regulators of respiratory chain function. *Mol. Cell* 2016. **63**: 621–632.

21 **Liu, G., Friggeri, A., Yang, Y., Park, Y.-J., Tsuruta, Y. and Abraham, E.**, miR-147, a microRNA that is induced upon Toll-like receptor stimulation, regulates murine macrophage inflammatory responses. *Proc. Natl. Acad. Sci. USA* 2009. **106**: 15819–15824.

22 **Gundra, U. M., Girgis, N. M., Ruckerl, D., Jenkins, S., Ward, L. N., Kurtz, Z. D., Wiens, K. E. et al.**, Alternatively activated macrophages derived from monocytes and tissue macrophages are phenotypically and functionally distinct. *Blood* 2014. **123**: e110–e122.

23 **Herbert, D. R., Hölscher, C., Mohrs, M., Arendse, B., Schwegmann, A., Radwanska, M., Leeto, M. et al.**, Alternative macrophage activation is essential for survival during schistosomiasis and downmodulates T helper 1 responses and immunopathology. *Immunity* 2004. **20**: 623–635.

24 **Cheever, A. W., Williams, M. E., Wynn, T. A., Finkelman, F. D., Seder, R. A., Cox, T. M., Hieny, S. et al.**, Anti-IL-4 treatment of *Schistosoma mansoni*-infected mice inhibits development of T cells and non-B, non-T cells expressing Th2 cytokines while decreasing egg-induced hepatic fibrosis. *J. Immunol.* 1994. **153**: 753–759.

25 **Coutinho, H. M., Acosta, L. P., Wu, H. W., Mcgarvey, S. T., Su, L., Langdon, G. C., Jiz, M. A. et al.**, Th2 cytokines are associated with persistent hepatic fibrosis in human *Schistosoma japonicum* infection. *J. Infect. Dis.* 2007. **195**: 288–295.

26 **Barron, L. and Wynn, T. A.**, Macrophage activation governs schistosomiasis-induced inflammation and fibrosis. *Eur. J. Immunol.* 2011. **41**: 2509–2514.

27 **Blankesteijn, W. M., Essers-Janssen, Y. P. G., Verluyten, M. J. A., Daemen, M. J. A. P. and Smits, J. F. M.**, A homologue of Drosophila tissue polarity gene frizzled is expressed in migrating myofibroblasts in the infarcted rat heart. *Nat. Med.* 1997. **3**: 541–544.

28 **Chera, S., Ghila, L., Dobretz, K., Wenger, Y., Bauer, C., Buzgariu, W., Martinou, J.-C. et al.**, Apoptotic cells provide an unexpected source of Wnt3 signaling to drive hydra head regeneration. *Dev. Cell.* 2009. **17**: 279–289.

29 **Weinstock, A., Rahman, K., Yaacov, O., Nishi, H., Menon, P., Nikain, C. A., Garabedian, M. L. et al.**, Wnt signaling enhances macrophage responses to IL-4 and promotes resolution of atherosclerosis. *Elife.* 2021. **10**.

30 **Miyoshi, H., Ajima, R., Luo, C. T., Yamaguchi, T. P. and Stappenbeck, T. S.**, Wnt5a potentiates TGF-beta signaling to promote colonic crypt regeneration after tissue injury. *Science* 2012. **338**: 108–113.

31 **Pull, S. L., Doherty, J. M., Mills, J. C., Gordon, J. I. and Stappenbeck, T. S.**, Activated macrophages are an adaptive element of the colonic epithelial progenitor niche necessary for regenerative responses to injury. *Proc. Natl. Acad. Sci. U S A* 2005. **102**: 99–104.

32 **Faas, M., Ipseiz, N., Ackermann, J., Culemann, S., Grüneboom, A., Schröder, F., Rothe, T. et al.**, IL-33-induced metabolic reprogramming controls the differentiation of alternatively activated macrophages and the resolution of inflammation. *Immunity* 2021. **54**: 2531–2546. e5.

33 **Bondurand, N., Dufour, S. and Pingault, V.**, News from the endothelin-3/EDNRB signaling pathway: Role during enteric nervous system development and involvement in neural crest-associated disorders. *Developmental Biology* 2018. **444**: S156–S169.

34 **Wong, N. R., Mohan, J., Kopecky, B. J., Guo, S., Du, L., Leid, J., Feng, G., Lokshina, I., Dmytrenko, O., Luehmann, H., Bajpai, G., Ewald, L., Bell, L., Patel, N., Bredemeyer, A., Weinheimer, C. J., Nigro, J. M., Kovacs, A., Morimoto, S., … Lavine, K. J.**, Resident cardiac macrophages mediate adaptive myocardial remodeling. *Immunity* 2021. **54**: 2072–2088.

35 **Jia, G. Q., Gonzalo, J. A., Lloyd, C., Kremer, L., Lu, L., Martinez-A, C., Wershil, B. K. and Gutierrez-Ramos, J. C.**, Distinct expression and function of the novel mouse chemokine monocyte chemotactic protein-5 in lung allergic inflammation. *The Journal of Experimental Medicine* **184**, 1939–1951.

36 **Seki, Y., Hayashi, K., Matsumoto, A., Seki, N., Tsukada, J., Ransom, J., Naka, T., Kishimoto, T., Yoshimura, A. and Kubo, M.**, Expression of the suppressor of cytokine signaling-5 (SOCS5) negatively regulates IL-4-dependent STAT6 activation and Th2 differentiation. *Proceedings of the National Academy of Sciences* 2002. **99**: 13003–13008.

37 **Smillie, C. S., Biton, M., Ordovas-Montanes, J., Sullivan, K. M., Burgin, G., Graham, D. B., Herbst, R. H. et al.**, Intra- and inter-cellular rewiring of the human colon during ulcerative colitis. *Cell* 2019. **178**: 714–730.e22.

38 **Hertati, A., Hayashi, S., Ogawa, Y., Yamamoto, T. and Kadowaki, M.**, Interleukin-4 receptor alpha subunit deficiency alleviates murine intestinal inflammation in vivo through the enhancement of intestinal mucosal barrier function. *Front Pharmacol* 2020. **11**: 573470.

39 **Stevceva, L., Pavli, P., Husband, A., Ramsay, A. and Doe, W.**, Dextran sulphate sodium-induced colitis is ameliorated in interleukin 4 deficient mice. *Genes Immun.* 2001. **2**: 309–316.

40 **Kim, H. S. and Chung, D. H.**, IL-9-producing invariant NKT cells protect against DSS-induced colitis in an IL-4-dependent manner. *Mucosal. Immunol.* 2013. **6**: 347–357.

41 **Hunter, M. M., Wang, A., Parhar, K. S., Johnston, M. J. G., Van Rooijen, N., Beck, P. L. and Mckay, D. M.**, In vitro-derived alternatively activated

macrophages reduce colonic inflammation in mice. *Gastroenterology* 2010. **138**: 1395–1405.

42 **Weisser, S. B., Kozicky, L. K., Brugger, H. K., Ngoh, E. N., Cheung, B., Jen, R., Menzies, S. C. et al.**, Arginase activity in alternatively activated macrophages protects PI3Kp110delta deficient mice from dextran sodium sulfate induced intestinal inflammation. *Eur. J. Immunol.* 2014. **44**: 3353–3367.

43 **Rossini, V., Zhurina, D., Radulovic, K., Manta, C., Walther, P., Riedel, C. U. and Niess, J. H.**, CX3CR1(+) cells facilitate the activation of CD4 T cells in the colonic lamina propria during antigen-driven colitis. *Mucosal. Immunol.* 2014. **7**: 533–548.

44 **Marelli, G., Belgiovine, C., Mantovani, A., Erreni, M. and Allavena, P.**, Non-redundant role of the chemokine receptor CX3CR1 in the anti-inflammatory function of gut macrophages. *Immunobiology* 2017. **222**: 463–472.

45 **Brunet, L. R., Finkelman, F. D., Cheever, A. W., Kopf, M. A. and Pearce, E. J.**, IL-4 protects against TNF-alpha-mediated cachexia and death during acute schistosomiasis. *J. Immunol.* 1997. **159**: 777–785.

46 **Schwartz, C., Oeser, K., Prazeres Da Costa, C., Layland, L. E. and Voehringer, D.**, T cell-derived IL-4/IL-13 protects mice against fatal *Schistosoma mansoni* infection independently of basophils. *J. Immunol.* 2014. **193**: 3590–3599.

47 **Pearce, E. J., Kane, C. M., Sun, J., Taylor, J. J., Mckee, A. S. and Cervi, L.**, Th2 response polarization during infection with the helminth parasite *Schistosoma mansoni*. *Immunol. Rev.* 2004. **201**: 117–126.

48 **Duffield, J. S., Lupher, M., Thannickal, V. J. and Wynn, T. A.**, Host responses in tissue repair and fibrosis. *Annu. Rev. Pathol.* 2013. **8**: 241–276.

49 **Gong, G.-C., Song, S.-R., Xu, X., Luo, Q., Han, Q., He, J.-X. and Su, J.**, Serpina3n is closely associated with fibrotic procession and knockdown ameliorates bleomycin-induced pulmonary fibrosis. *Biochem. Biophys. Res. Commun.* 2020. **532**: 598–604.

50 **Karpus, O. N., Westendorp, B. F., Vermeulen, J. L. M., Meisner, S., Koster, J., Muncan, V., Wildenberg, M. E. et al.**, Colonic CD90+ Crypt fibroblasts secrete semaphorins to support epithelial growth. *Cell Rep.* 2019. **26**: 3698–3708. e5.

51 **Bosurgi, L., Bernink, J. H., Delgado Cuevas, V., Gagliani, N., Joannas, L., Schmid, E. T., Booth, C. J. et al.**, Paradoxical role of the proto-oncogene Axl and Mer receptor tyrosine kinases in colon cancer. *Proc. Natl. Acad. Sci. USA* 2013. **110**: 13091–13096.

52 **Cummings, R. J., Barbet, G., Bongers, G., Hartmann, B. M., Gettler, K., Muniz, L., Furtado, G. C. et al.**, Different tissue phagocytes sample apoptotic cells to direct distinct homeostasis programs. *Nature* 2016. **539**: 565–569.

53 **Schridde, A., Bain, C. C., Mayer, J. U., Montgomery, J., Pollet, E., Denecke, B., Milling, S. W. F. et al.**, Tissue-specific differentiation of colonic macrophages requires TGFbeta receptor-mediated signaling. *Mucosal. Immunol.* 2017. **10**: 1387–1399.

54 **Goenka, S. and Kaplan, M. H.**, Transcriptional regulation by STAT6. *Immunol. Res.* 2011. **50**: 87–96.

55 **Hoeksema, M. A., Shen, Z., Holtman, I. R., Zheng, A., Spann, N. J., Cobo, I., Gymrek, M. et al.**, Mechanisms underlying divergent responses of genetically distinct macrophages to IL-4. *Sci. Adv.* 2021. **7**.

56 **Kimura, A., Naka, T., Nakahama, T., Chinen, I., Masuda, K., Nohara, K., Fujii-Kuriyama, Y. et al.**, Aryl hydrocarbon receptor in combination with Stat1 regulates LPS-induced inflammatory responses. *J. Exp. Med.* 2009. **206**: 2027–2035.

57 **Bosurgi, L., Cao, Y. G., Cabeza-Cabrerizo, M., Tucci, A., Hughes, L. D., Kong, Y., Weinstein, J. S. et al.**, Macrophage function in tissue repair and remodeling requires IL-4 or IL-13 with apoptotic cells. *Science* 2017. **356**: 1072–1076.

58 **Lin, J.-D., Nishi, H., Poles, J., Niu, X., Mccauley, C., Rahman, K., Brown, E. J. et al.**, Single-cell analysis of fate-mapped macrophages reveals heterogeneity, including stem-like properties, during atherosclerosis progression and regression. *JCI Insight* 2019. **4**.

59 **Zimmer, A., Bouley, J., Le Mignon, M., Pliquet, E., Horiot, S., Turfkruyer, M., Baron-Bodo, V. et al.**, A regulatory dendritic cell signature correlates with the clinical efficacy of allergen-specific sublingual immunotherapy. *J. Allergy Clin. Immunol.* 2012. **129**: 1020–1030.

60 **Salcher, S., Sturm, G., Horvath, L., Untergasser, G., Kuempers, C., Fotakis, G., Panizzolo, E. et al.**, High-resolution single-cell atlas reveals diversity and plasticity of tissue-resident neutrophils in non-small cell lung cancer. *Cancer Cell* 2022. **40**: 1503–1520. e8.

61 **Bates, J. and Diehl, L.**, Dendritic cells in IBD pathogenesis: an area of therapeutic opportunity? *J. Pathol.* 2014. **232**: 112–120.

62 **Fournier, B. M. and Parkos, C. A.**, The role of neutrophils during intestinal inflammation. *Mucosal. Immunol.* 2012. **5**: 354–366.

63 **Everts, B., Hussaarts, L., Driessen, N. N., Meevissen, M. H. J., Schramm, G., Van Der Ham, A. J., Van Der Hoeven, B. et al.**, Schistosome-derived omega-1 drives Th2 polarization by suppressing protein synthesis following internalization by the mannose receptor. *J. Exp. Med.* 2012. **209**: 1753–1767. S1.

64 **Klaver, E. J., Kuijk, L. M., Lindhorst, T. K., Cummings, R. D. and Van Die, I.**, *Schistosoma mansoni* soluble egg antigens induce expression of the negative regulators SOCS1 and SHP1 in human dendritic cells via interaction with the mannose receptor. *PLoS One* 2015. **10**: e0124089.

65 **Chuah, C., Jones, M. K., Burke, M. L., Mcmanus, D. P., Owen, H. C. and Gobert, G. N.**, Defining a pro-inflammatory neutrophil phenotype in response to schistosome eggs. *Cell Microbiol.* 2014. **16**: 1666–1677.

66 **Becker, C., Fantini, M. C. and Neurath, M. F.**, High resolution colonoscopy in live mice. *Nat. Protoc.* 2006. **1**: 2900–2904.

67 **Dobin, A., Davis, C. A., Schlesinger, F., Drenkow, J., Zaleski, C., Jha, S., Batut, P. et al.**, STAR: ultrafast universal RNA-seq aligner. *Bioinformatics* 2013. **29**: 15–21.

68 **Robinson, M. D., Mccarthy, D. J. and Smyth, G. K.**, edgeR: a Bioconductor package for differential expression analysis of digital gene expression data. *Bioinformatics* 2010. **26**: 139–140.

Abbreviations: **ALT**: alanine aminotransaminase · **BMDMs**: bone marrow-derived macrophages · **CX3CR1**: CX3 chemokine receptor 1 · **DEGs**: differentially expressed genes · **DSS**: dextran sodium sulfate · ***Nmes1***: normal mucosa of esophagus-specific gene 1 · **UC**: ulcerative colitis

Full correspondence: Dr. Lidia Bosurgi, I. Department of Medicine, Hamburg Center for Translational Immunology, University Medical Center Hamburg-Eppendorf, 20246 Hamburg, Germany
e-mail: l.bosurgi@uke.de

Received: 15/2/2023
Revised: 14/11/2023
Accepted: 15/11/2023
Accepted article online: 16/11/2023